HHS Public Access

Author manuscript

*Int J Hyperthermia*. Author manuscript; available in PMC 2019 December 01.

Published in final edited form as:

*Int J Hyperthermia*. 2018 December ; 34(8): 1186–1193. doi:10.1080/02656736.2018.1447149.

# High Power Microwave Ablation of Normal Swine Lung: Impact of Duration of Energy Delivery on Adverse Event and Heat Sink Effects

**Hiroshi Kodama, MD**[1], **Eisuke Ueshima, MD, PhD**[1], **Song Gao, MD**[1], **Sebastien Monette, DMV**[2], **Lee-Ronn Paluch, BVSc**[3], **Kreg Howk, MS**[4], **Joseph P Erinjeri, MD, PhD**[1,5], **Stephen B Solomon, MD**[1,5], and **Govindarajan Srimathveeravalli, PhD**[1,4]

[1]Department of Radiology, Interventional Radiology Service, Memorial Sloan-Kettering Cancer Center 1275 York Avenue, New York, NY, 10065

[2]Laboratory of Comparative Pathology, Memorial Sloan Kettering Cancer Center, The Rockefeller University, Weill Cornell Medicine, New York, USA.

[3]Center of Comparative Medicine and Pathology, Memorial Sloan Kettering Cancer Center, Weill Cornell Medicine, Hospital for Special Surgery, New York, USA

[4]Medtronic Inc., Massachusetts, USA.

[5]Department of Radiology, Weill Cornell Medical College. New York, USA.

## Abstract

**Purpose:** To assess the impact of duration of energy delivery on adverse events (AEs) and heat sink effects during high power microwave ablation (MWA) of normal swine lung.

**Materials and Methods:** High power (100 Watts) MWA was performed with short (2 minutes, 18 ablations) or long (10 minutes, 9 ablations) duration of energy delivery in unilateral lung of swine (n=10). CT imaging was done prior to sacrifice at 2 or 28 days post-treatment, with additional imaging at 7 and 14 days for the latter cohort. Ablation zones were assessed with CT imaging and histopathology analysis. Differences in AEs and ablation characteristics between groups were compared with Fisher's exact test and Student's t-test, respectively.

**Results:** There were no significant differences in formation of air-filled needle tract, cavitation, and pneumonia ($p$>0.5) between the treatment groups. Intra-procedural pneumothorax requiring chest tube placement occurred in 3 animals. Substantial (>20%, *p=0.01)* intra-procedural ablation zone distortion was observed in both groups. Presence of large airways or blood vessels did not result in heat sink effect within the ablation zones and was not indicative of reduced ablation size. Increased energy delivery yielded larger (8.9±3.1cm$^3$ vs 3.4±1.7 cm$^3$, $p$<0.001) spherical ablations (sphericity: 0.70±0.10 vs.0.56±0.13, $p$=0.01).

Corresponding author: Govindarajan Srimathveeravalli, H112, Dept. of Radiology, 1275 York Avenue, New York, NY, 10065, 1-212-639-3297, srimaths@mskcc.org.

DECLARATION OF CONFLICT OF INTEREST

The other authors have no conflict of interests to report regarding the work reported in this manuscript.

**Conclusion:** High power MWA of normal lung with longer duration of energy delivery can create larger spherical ablations, without significant differences in post-procedure AEs when compared with shorter energy delivery time.

### Keywords

microwave ablation; lung; preclinical animal study; adverse event; heat sink effect

## INTRODUCTION

Thermal ablation with microwave or radiofrequency energy has emerged as an efficacious treatment option for unresectable lung tumors, and has been used to treat both primary and secondary thoracic malignancies [1, 2, 3, 4, 5, 6, 7]. Microwave ablation (MWA) at high power (100 – 180 W) is capable of rapid destruction of both small and large tumors with single or multiple applicators [3, 4, 5, 6, 7]. High power MWA may also potentially provide a more complete ablative margin by reducing the heat sink effects of large blood vessels [8, 9]. Despite these potential benefits, the clinical rationale to apply longer durations of high power energy delivery in the lung with a single applicator is unclear due to limited information on the associated risks and benefits.

Clinical studies report that MWA performed even at low power settings (10– 80 W) can cause adverse effects such as pneumothorax [10, 11, 12, 13, 14], bleeding [15], bronchopleural fistula [14], and air leak [16]. MWA has been attempted at high power, at 80–120W[5, 6, 7] and 180 W [3], albeit with energy delivery for a short duration (under 4 minutes for a single applicator). Despite the short duration of energy delivery, pneumothorax requiring a chest tube has been reported in 13 [7]-20% [6] of these cases. Furthermore, MWA at high power can rapidly elevate tissue temperature (100°C in less than a minute), resulting in desiccation, distortion or contraction of tissue within the ablation in ex vivo lung and liver [17]. Hence, there is a need to assess the in vivo dynamics of intra-procedural pulmonary parenchyma/tissue distortion within the ablation site, and clarify the risks and benefits associated with high power MWA delivered at long durations. The purpose of this study was to evaluate high power MWA in an in vivo normal swine lung model and to assess the impact of duration of energy delivery on adverse events (AE) and heat sink effects.

## MATERIALS AND METHODS

Studies were performed in a swine lung model in vivo with the Emprint™ Ablation System incorporating the Thermosphere™ Technology (Medtronic, Boulder, Colorado) in a prospective study approved by the Institutional Animal Care and Use Committee. The Thermosphere MWA system (2,450 Mhz/100W) was designed to produce spherical zones of ablation based on three types of energy control (thermal, field, and wavelength control) [18].

### Study design

The primary endpoint of this study was incidence of AEs comparing short (2 minutes, 12 kJ) versus long (10 minutes, 60 kJ) duration of energy delivery at a generator power output of 100 W. The device has an estimated cable efficiency of 60% or cable attenuation of 40%.

The 10-minute ablation was considered ‘high’ dose and the 2-minute ablation was considered ‘low’ dose. The experimental energy delivery durations were chosen to approximately match the lower (17 kJ) and higher (52 kJ) total energy used to perform MWA of lung tumors in patients. Secondary endpoints of the study were the incidence of heat sink effects and the dose-dependent variations in ablation shape and size.

## In Vivo Porcine Lung Ablation

Ten male swine (3–4 months old; weight range, 50–70 kg) were used in the study. The animals were sedated, and general anesthesia was maintained using continuous inhalation of isoflurane while percutaneous MWA was performed in unilateral swine lung (right lung in one animal, left lung in the remaining animals). CT imaging (Lightspeed RTLS, GE Healthcare, Milwaukee, Wl) was used for insertion of 2 or 3 antennas per animal, and each antenna was used to create a single ablation. Antenna insertion was synchronous, and energy delivery was performed sequentially one antenna at a time for each ablation. In total, twenty-seven sites were treated at 2450 MHz and 100 W, for either 2 minutes (low dose, 18 ablations in 10 animals) or 10 minutes (high dose, 9 ablations in 9 animals). Intra-procedural AEs were collected by monitoring vital signs and through CT fluoroscopy performed at one-minute intervals. Animals that demonstrated post-ablation pneumothorax underwent additional imaging up to 2 hours post-treatment. Chest tube placement was performed only in animals with worsening pneumothorax. Animals were euthanized through an intravenous overdose of pentobarbital at 2 (n=5) or 28 (n=5) days post-ablation.

## CT Imaging and Measurements

Non-contrast and dual-phase (30s and 90s) CT imaging with contrast (Omnipaque 300 mg/ml; GE Healthcare, Princeton, NJ; 4 ml/s; 2 cc/kg; using auto injector) was performed before, during, and within 10 minutes of ablation, and at 2, 7, 14 and 28 days post-ablation. Imaging parameters were as follows: tube voltage of 120 kV, tube current as determined by automatic exposure control, CT gantry rotation time of 0.8sec, pitch factor of 0.9375, image slice thickness of 1.25 mm, and data collection diameter of 500 mm. The ablation zone on CT was defined as the region demonstrating ground-glass opacity enclosed within a hyperdense rim on lung window settings, and as a non-enhancing region on the mediastinal window setting. Figure 1 shows the serial change of CT image following MWA with short- and long-duration energy delivery. Treatment-related AEs, including pneumothorax, hemorrhage, pneumonia, and cavitation seen on CT were recorded. When consolidation was observed at a site other than the ablation zone and elevation of body temperature was detected, it was defined as pneumonia. Air density area within the ablated parenchyma, which was differentiated from antenna tract or airway, was defined as cavitation. Rapid heating and high tissue temperatures during MWA induce rapid desiccation, causing distortion of the ablated tissue. Three separate measurements were performed on CT images acquired immediately before and after each ablation to record MWA-related distortion of lung tissue (See Appendix 1 for details). The distortion ratio was calculated using the formula: Distortion ratio = $(Db\text{-}Da)/Db$ where $Da$ and $Db$ were the distance between anatomic landmarks and the center of the ablation probe measured immediately after or before the ablation, respectively. Ablation zone sphericity was calculated using the following

formula: Sphericity = Short-axis diameter/Long-axis diameter. Perfect sphere was indicated by sphericity of 1.

### Pathology Analysis

Immediately following euthanasia at days 2 and 28, the trachea and both lungs were removed en-bloc and were formalin-fixed using a gravity assisted fixation technique (See Appendix 2 for information on the procedure used for pathology sample and slide preparation). Large slides were prepared to capture the entire ablation zone corresponding to the largest cross-section on imaging. H&E stained samples were evaluated by a board-certified veterinary pathologist (S.M.) for evidence of AEs such as airway fistula, severe hemorrhage, loss of tissue integrity, and vascular injury. Measurements of the maximum width of hyperemic rim or fibrotic rim, maximum diameter of completely ablated bronchus or vessel inside the ablation zone, and minimum diameter of incompletely ablated bronchus or vessel at the ablation margin were also performed.

### Adverse Event Assessment

Adverse event (AE) was assessed based on Society of Interventional Radiology (SIR) classification. Major complication was defined as an event that led to substantial morbidity and disability, increasing the level of care [19]. All other complications were considered minor. Adverse event assessments were performed through regular clinical assessments of the animal by an experienced staff veterinarian (L.P), and by the investigators (H.K. and E.U.) during planned intra- and post-procedural CT follow-up imaging.

### Statistics

Frequency of AEs on CT was compared between short and long duration treatments using Fisher's exact test. Ablation zone size, sphericity, distortion ratio, and the diameter of bronchus/vessels inside the ablation zone or at the ablation margin were compared between short and long duration treatments using Student's *t* test. The distortion ratio was compared between pre- and post-treatment shift of anatomical features within and outside the ablation zone, and with the contralateral lung. All statistical analyses were conducted using EZR software (Saitama Medical Center, Jichi Medical University, Saitama, Japan), which is a graphical user interface for R (The R Foundation for Statistical Computing, Vienna, Austria) (26). A $p$-value of$<0.05$ was inferred as indicating a significant difference between measurements.

## RESULTS

### The duration of energy delivery does not impact incidence or severity of adverse events seen on CT imaging

The major treatment-related AE was intraprocedural pneumothorax requiring chest tube placement, which occurred in 3 of 10 animals (Table 1). Continuous air drainage with wall suction was necessary to maintain lung expansion in 2 animals, while the pneumothorax stabilized without suction in 1 animal. Pneumothorax in the latter animal was controlled using a flutter valve and was observed to resolve on CT imaging on day 2 post-ablation. Resource and experimental constraints did not permit continuous wall suction in 2 of 3

animals, and they were euthanized within four hours after MWA. Data acquired with these animals were included only for evaluation of intra-procedural AE.

Minor post-procedural AEs occurred in 6 of 10 animals, including pneumothorax not requiring chest tube placement (n=6), cavitation within the ablation zone (n=1), and pneumonia (n=2) (Table 1). Minor pneumothoraces were typically observed within 10 minutes post-ablation. Cavitation completely enclosed within the ablation site was observed with CT imaging at 7-day follow-up in a single animal. The cavitation reduced in size without additional intervention. Pneumonia was observed in 2 animals at 7-day follow-up on both CT imaging and through clinical assessment of symptoms (high temperatures in both animals; coughing and appetite loss in one animal). Both animals recovered after treatment with antibiotics (ceftiofur, 3 mg/kg, oral once daily for 3 days). There were no significant differences in cavitation (p=1.0) and pneumonia (p=1.0) between the long and short-duration energy treatment groups.

### The duration of energy delivery does not affect the formation of air-filled needle tract

For the 2 animals with pneumothorax requiring chest tube placement and receiving continuous air drainage with wall suction (Table 1), CT images revealed the formation of a visible needle tract along the path of ablation probe placement, which allowed passage of air from the lung into the pleural space (Figure 2a). Such tract was present in a low dose ablation site in one animal, and in a high dose ablation site in another animal. Similar air-filled needle tracts were observed in 18.5% of all ablations, however these tracts did not appear to allow passage of air into the pleural space. Such tracts were observed in 16.7% ablations performed at low energy dose and in 22.2% of the high dose ablations, but the difference was not found to be statistically significant ($p$=0.99) (Table 2). Histologic examinations of such air-filled needle tracts revealed no evidence of thermal injury at the site of the needle tract. The presence of air-filled needle tract or passage of air to the pleura was not observed in animals with minor pneumothorax (Table 1).

### Increasing the duration of energy delivery does not reduce heat sink effect at the ablation boundary

Tissue samples from the two swine that were sacrificed acutely were not included for evaluation of heat sink effect on histology samples. Comparison of histopathological findings were performed using 22 specimens from 8 animals: 4 long duration and 6 short duration ablations from animals sacrificed 2 days post-ablation (n=4), and 4 long duration and 8 short duration ablations from animals sacrificed at 28 days post-ablation (n=4). All examined airways and blood vessels within the ablation zone appeared completely necrotic in samples from both treatment groups at the 2-day time point. The maximal diameter of airways and blood vessels observed within ablations zones were 5.1 mm and 4.1 mm, respectively. The mean diameter of airways and blood vessels within the ablation zone was not significantly different between the two treatment groups (Table 3). Airways and blood vessels at the ablation boundary demonstrated incomplete necrosis in both treatment groups. Occasional evidence of concave distortion of ablation margin consistent with heat sink effect was seen in samples from days 2 and 28 in both treatment groups (Figure 3f). The mean

diameter of airways and blood vessels showing incomplete necrosis at the edge of ablation zone was not significantly different between the two treatment groups (Table 3).

### MWA induces significant intra-procedural distortion of lung parenchyma within the ablation

Following MWA, there were considerable changes in the position of anatomic landmarks (such as blood vessels and airways) within the ablation site when measured relative to the microwave probe. The change in anatomical landmark position was consistent with distortion or contraction of tissue, which was significant when compared to untreated parenchyma outside the ablation or equivalent measurements performed on the contralateral lung (Figure 4). The distortion ratio calculated for the ablation zone was 19.9±20.1 while equivalent measurements made in the contralateral lung was 1.9±4.1 ($p$<0.01). The relative position of anatomical landmarks outside the ablation and the center of the ablation did not demonstrate significant change ($p$=0.86), suggesting the distortion effect to be limited to the ablation. The distortion ratio was not significantly different between short (18±22) and long (24±18) duration energy delivery ($p$=0.38).

### Longer duration MWA yielded larger and more spherical ablations relative to shorter duration of energy delivery

Ablation size of longer duration treatments was significantly larger than shorter duration treatments (Table 2, Figure 1). Longer energy delivery also duration produced more spherical ablation zones when compared with shorter duration energy delivery (Table 2). Increased duration of energy delivery was associated with greater increase (76.7%) in the short axis diameter of the ablation zone when compared to change in the long axis diameter (37.5%). This finding may underlie the increased size and sphericity observed in long-duration ablations. Using Pearson's coefficient analysis, the maximum diameter of ablated bronchus or vessels on pathological specimen did not correlate with ablation zone size on pathological specimen both at day 2 (airway, p=0.14 [long] and 0.25 [short], vessel, p=0.25 [long] and 0.66 [short]) and day 28 (airway, p=0.16 [long] and 0.13 [short], vessel, p=0.61 [long] and 0.18 [short]), suggesting that heat sink effects do not affect or reduce ablation size.

### Histologic patterns of tissue injury and healing are similar following short and long duration ablations

Common findings at day 2 included a well-demarcated area of complete coagulation necrosis of all structures (alveoli, airways, blood vessels), with a rim of hyperemia, hemorrhage, and fibrin exudation in the peripheral portion of the necrotic zone (Figure 3a). Variable thermal change, including basophilic discoloration of collagen, was present within the area of necrosis. At day 28, common findings included a well-demarcated area of complete coagulation necrosis and multifocal calcification of all structures, surrounded by a rim of dense fibrosis and inflammation characterized by infiltration of numerous neutrophils, macrophages, lymphocytes, and plasma cells (Figure 3b). The calcification observed on H&E stained slides was microscopic, and was not detected on CT images. Airway and blood vessel perforation were not observed in any of the samples. The architecture of the necrotic bronchi was maintained at day 2 (Figure 3d). There was no evidence of airway regeneration

or recovery within the ablation zone in either treatment group at day 28 (Figure 3e). Width of the hyperemic inflammatory rim at the ablation margin at day 2, and the fibrotic rim at day 28 were not significantly different between short and long duration ablations (Table 3). Overall, histologic findings and the appearances of cavitation and other features appeared remarkably similar in samples from both ablation groups.

## DISCUSSION

The results of this study did not reveal any significant differences in the incidence or severity of AEs based on the duration of energy delivery during high power MWA in the lung. Results also suggest that the major benefit of increasing the duration of energy delivery is the creation of ~3 cm spherical ablations with a single applicator. Increasing the duration of energy delivery provides more time for heat convection through tissue and thereby may have contributed to increasing ablation size radial to the applicator, creating ablations that were more spherical in shape. A five-fold increase in the duration of energy delivery yielded roughly a three-fold increase in ablation volume, for short and long duration treatments respectively, suggesting a proportional relationship between energy delivered and ablation volume. MWA generators employ different energy delivery strategies, and our results should be considered specific to the generator/antenna combination that we have tested.

Results from this study show that the MWA appears to be well-tolerated. Three animals had pneumothorax that required chest tube placement; pneumothorax was eventually stabilized in all 3 animals. The experimental design of study, where 2–3 ablations were performed in each animal, is not common in clinical practice, and may have inadvertently increased the incidence of pneumothorax. CT imaging immediately after the ablation revealed formation of air-filled needle tract in 26% of ablations, including 2 cases with passage of air into the pleural space. The duration of energy delivery did not influence incidence or severity of this finding. Passage of air through the needle tract to the pleura was identified as the underlying cause of pneumothorax in some of the animals. While the etiology of air-filled needle tract is unclear, this complication may be prevented by adjusting the approach of the probe placement [20] and ensuring at least a 2 cm spacing between the boundary of the served ablation zone and the pleural surface [21]. The incidence of cavitation observed in our study was much lower than the incidence rate (43%) reported by Wolf et al. [22] in patients undergoing MWA of lung tumors. Hence, ablation of the normal lung may be less prone to cavitation than tumors that may already be largely necrotic. Cavitation within the ablation can have both favorable and unfavorable implications. It has been attributed as a significant indicator of reduced cancer-specific mortality in patients [22], but at the same time can increase the possibility of infection and pneumonia [23]. In our study, 1 of 2 animals with pneumonia had cavitation within the ablation, which may have contributed to the development of pneumonia. This study was performed with a single device, and AE arising from the trauma of applicator placement was not studied. Our reported AE profile may not be extensible to other applicators having a different diameter or trocar profile. Likewise, other AEs such as skin or chest wall burns are closely related to the control of energy delivery at the antenna. While our study does not report such incidents, it is unknown whether energy delivery with other device/generator combinations will result in similar outcomes.

In an ex vivo study by Brace et al. [17], where ablations were performed at low power energy settings (40 W for 10 minutes), it was reported that normal lung tissue contracted 15%−50% after MWA. The lung tissue inside the ablation zone contracted significantly within the ablation zone in a heterogeneous fashion without any significant difference between the two treatment groups. However, it must be noted that even within each ablation cohort, significant variation was observed in the measured distortion ratio, and the underlying reasons are not readily apparent. While it is evident that MWA ablation can induce significant distortion in the lung, predicting the extent of distortion at this point remains a challenge. Furthermore, placement of the antenna itself can distort regional anatomy, and sham-controlled measurements were not performed to quantify this effect. As all measurements were performed following antenna placement in both low and high dose groups, we anticipate its contribution to the final distortion in the treated lung to be similar for all samples. Distortion effects were present only within the ablation and were not observed in normal lung outside the ablation zone. This differential effect suggests that heat sensitive structures such as the heart, nerves or pleura will be safe from the effects of MWA-related distortion as long as the ablation is planned such that these structures remain outside the region receiving treatment.

In this study, all bronchi and blood vessels were observed within the ablation zone and were completely necrotic, regardless of size and the duration of energy delivery. This suggests that tissue temperature during ablation, and not the total time of energy delivery, may be crucial to overcome the protective effects of heat sinks within the ablation. However, this finding does not extend to the ablation boundary as incomplete ablation or concave distortion of the ablation was found in histologic samples of both treatment groups. Therefore, adjusting probe placement to include all blood vessels and the airway within the ablation zone may be crucial to obtaining good margins during MWA of the lung.

The ability of high power MWA to influence the size of the post-ablation inflammatory rim and subsequent immunologic response was the subject of a recent study [24]. The histologic findings of this study indicate that duration of energy delivery does not affect the size of the inflammatory rim in the acute setting and the fibrotic rim during longer term follow-up. Microscopic calcifications were observed in a number of tissue samples on histology, and examination of peripheral tissue suggest this may be the result of increased activity of macrophages clearing tissue debris at the ablation site. Overall, high power MWA of lung tumors may allow complete tumor eradication while preserving immunologic benefits associated with thermal ablation.

This study has several limitations. Ablations were performed in normal lung rather than tumor; the absence of representative tumor models remains a significant limitation of most preclinical large animal studies. The animals that were ablated in this study were young animals and in robust health; older patients with co-morbidities and tumor burden may be more prone to AEs. Distortion of lung tissue was evaluated only via CT imaging. Since multiple ablations were performed in each animal, this design does not allow accurate identification of the energy setting that may have caused pneumothorax.

## CONCLUSION

In conclusion, the duration of energy delivery during high power lung ablation does not seem to increase the overall risk of ablation-related AEs in a porcine model. The absence of heat sink effect and complete tissue destruction within the ablation zone during MWA is independent of the duration of energy delivery, supporting longer energy delivery to achieve good ablation margins. The number of interventions in each animal, and the ablation size may also have contributed to reported AEs, and must be taken in consideration when translating our findings to patient treatment.

## ACKNOWLEDGEMENT

The authors acknowledge the support of NIH Cancer Center Support Grant (P30 CA008748) for core laboratory services used for the experimental studies. Medical writing support was provided by Mamata Thapa, PhD (Medtronic).

G.S. received grant support from Medtronic Inc. to perform the reported work. K.H. is an employee of Medtronic Inc. but was not directly involved in study design, data collection or analysis of results.

## Appendix 1: Measurements for evaluating lung distortion in this study

| |
|---|
| The following measurements were performed on CT images to assess lung distortion:<br>• Distance between the center of the ablation zone (low density point on probe) and landmark bronchus/vessel (≥2 mm in diameter) present within the ablation.<br>• Distance between the center of the ablation zone and a landmark bronchus/vessel (≥2 mm in diameter) outside the ablation.<br>• Distance between bronchi or vessels and fixed anatomical landmarks in contralateral untreated lung. |
| Measurements in contralateral lung were used to compensate for respiratory motion |
| The landmark used for measurements on the blood vessel or bronchi was chosen by the presence of anatomical features such as a bifurcation or other unique CT imaging feature |
| Ablations where suitable anatomic landmarks matching our criterion were not found were excluded from evaluation |

## Appendix 2: Procedure for pathology slide preparation

| | |
|---|---|
| 1. | An endotracheal intubation tube was placed into the trachea, and whole lungs were fixed by instillation of 10% neutral buffered formalin (NBF) solution into the airway with pressure of 0.04 MPa for 30 minutes. |
| 2. | Following fixation, the treated lung was examined to identify needle insertion tracts, and ablation zones were sectioned parallel to the tract when identified. |
| 3. | The entire lung was step-sectioned at 3–5 mm intervals when the needle path could not be observed. |
| 4. | The representative ablation sections were fixed in 10% NBF solution, processed routinely in ethanol and xylene, embedded in paraffin, sectioned at 4-μm thickness, and stained with hematoxylin and eosin. |
| 5. | The largest cross section of each ablation with surrounding untreated lung parenchyma was captured in large histology slides. |

## REFERENCES

1. Yamakado K, Hase S, Matsuoka T, et al. Radiofrequency ablation for the treatment of unresectable lung metastases in patients with colorectal cancer: a multicenter study in Japan. J Vasc Interv Radiol. 2007 3;18(3):393–8. doi: 10.1016/j.jvir.2006.11.003. PubMed PMID: . [PubMed: 17377185]

2. Alexander ES, Dupuy DE. Lung cancer ablation: technologies and techniques. Semin Intervent Radiol. 2013 6;30(2):141–50. doi: 10.1055/S-0033-1342955. PubMed PMID: ; PubMed Central PMCID: PMCPMC3709947. [PubMed: 24436530]

3. Little MW, Chung D, Boardman P, et al. Microwave ablation of pulmonary malignancies using a novel high-energy antenna system. Cardiovasc Intervent Radiol. 2013 4;36(2):460–5. doi: 10.1007/s00270-012-0465-2. PubMed PMID: . [PubMed: 22968596]

4. Liu H, Steinke K. High-powered percutaneous microwave ablation of stage I medically inoperable non-small cell lung cancer: a preliminary study. J Med Imaging Radiat Oncol. 2013 8;57(4):466–74. doi: 10.1111/1754-9485.12068. PubMed PMID: . [PubMed: 23870347]

5. lerardi AM, Coppola A, Lucchina N, et al. Treatment of lung tumours with high-energy microwave ablation: a single-centre experience. Med Oncol. 2017 1;34(1):5. doi: 10.1007/s12032-016-0861-6. PubMed PMID: . [PubMed: 27900591]

6. Egashira Y, Singh S, Bandula S, et al. Percutaneous High-Energy Microwave Ablation for the Treatment of Pulmonary Tumors: A Retrospective Single-Center Experience. J Vasc Interv Radiol. 2016 4;27(4):474–9. doi: 10.1016/j.jvir.2016.01.001. PubMed PMID: . [PubMed: 26944360]

7. Splatt AM, Steinke K. Major complications of high-energy microwave ablation for percutaneous CT-guided treatment of lung malignancies: Single-centre experience after 4 years. J Med Imaging Radiat Oncol. 2015 10;59(5):609–16. doi: 10.1111/1754-9485.12345. PubMed PMID: . [PubMed: 26238653]

8. Liang P, Yu J, Lu MD, et al. Practice guidelines for ultrasound-guided percutaneous microwave ablation for hepatic malignancy. World J Gastroenterol. 2013 9 07;19(33):5430– 8. doi: 10.3748/wjg.v19.i33.5430. PubMed PMID: ; PubMed Central PMCID: PMCPMC3761095. [PubMed: 24023485]

9. Dou JP, Yu J, Yang XH, et al. Outcomes of microwave ablation for hepatocellular carcinoma adjacent to large vessels: a propensity score analysis. Oncotarget. 2017 Apr 25;8(17):28758– 28768. doi: 10.18632/oncotarget. 15672. PubMed PMID: ; PubMed Central PMCID: PMCPMC5438689. [PubMed: 28430634]

10. Ko WC, Lee YF, Chen YC, et al. CT-guided percutaneous microwave ablation of pulmonary malignant tumors. J Thorac Dis. 2016 Oct;8(Suppl 9):S659–S665. doi: 10.21037/jtd.2016.09.44. PubMed PMID: ; PubMed Central PMCID: PMCPMC5179347. [PubMed: 28066666]

11. Vogl TJ, Naguib NN, Gruber-Rouh T, et al. Microwave ablation therapy: clinical utility in treatment of pulmonary metastases. Radiology. 2011 Nov;261(2):643–51. doi: 10.1148/radiol.11101643. PubMed PMID: . [PubMed: 22012906]

12. Belfiore G, Ronza F, Belfiore MP, et al. Patients' survival in lung malignancies treated by microwave ablation: our experience on 56 patients. Eur J Radiol. 2013 1;82(1):177–81. doi: 10.1016/j.ejrad.2012.08.024. PubMed PMID: . [PubMed: 23099201]

13. Lu Q, Cao W, Huang L, et al. CT-guided percutaneous microwave ablation of pulmonary malignancies: Results in 69 cases. World J Surg Oncol. 2012 May 07;10:80. doi: 10.1186/1477-7819-10-80. PubMed PMID: ; PubMed Central PMCID: PMCPMC3407730. [PubMed: 22564777]

14. Zheng A, Wang X, Yang X, et al. Major complications after lung microwave ablation: a single-center experience on 204 sessions. Ann Thorac Surg. 2014 7;98(1):243–8. doi: 10.1016/j.athoracsur.2014.03.008. PubMed PMID: . [PubMed: 24793688]

15. Liang P, Wang Y, Yu X, et al. Malignant Liver Tumors: Treatment with Percutaneous Microwave Ablation—Complications among Cohort of 1136 Patients. Radiology. 2009;251(3):933–940. doi: 10.1148/radiol.2513081740. PubMed PMID: . [PubMed: 19304921]

16. Simon CJ, Dupuy DE, Mayo-Smith WW. Microwave Ablation: Principles and Applications. RadioGraphics. 2005;25(suppl_1):S69–S83. doi: 10.1148/rg.25si055501. PubMed PMID: . [PubMed: 16227498]

17. Brace CL, Diaz TA, Hinshaw JL, et al. Tissue contraction caused by radiofrequency and microwave ablation: a laboratory study in liver and lung. J Vasc Interv Radiol. 2010 8;21(8):1280–6. doi: 10.1016/j.jvir.2010.02.038. PubMed PMID: ; PubMed Central PMCID: PMCPMC2920145. [PubMed: 20537559]

18. Alonzo M, Bos A, Bennett S, et al. The Emprint Ablation System with Thermosphere Technology: One of the Newer Next-Generation Microwave Ablation Technologies. Semin Intervent Radiol. 2015 Dec;32(4):335–8. doi: 10.1055/S-0035-1564811. PubMed PMID: ; PubMed Central PMCID: PMCPMC4640908. [PubMed: 26622094]

19. Ahmed M, Solbiati L, Brace CL, et al. Image-guided tumor ablation: standardization of terminology and reporting criteria--a 10-year update. J Vasc Interv Radiol. 2014 11;25(11): 1691–705 e4. doi: 10.1016/j.jvir.2014.08.027. PubMed PMID: . [PubMed: 25442132]

20. Lee KS, Takaki H, Yarmohammadi H, et al. Pleural puncture that excludes the ablation zone decreases the risk of pneumothorax after percutaneous microwave ablation in porcine lung. J Vasc Interv Radiol. 2015 7;26(7): 1052–8. doi: 10.1016/j.jvir.2015.01.016. PubMed PMID: . [PubMed: 25753501]

21. Hinshaw JL, Lubner MG, Ziemlewicz TJ, et al. Percutaneous tumor ablation tools: microwave, radiofrequency, or cryoablation--what should you use and why? Radiographics. 2014 Sep-Oct; 34(5):1344–62. doi: 10.1148/rg.345140054. PubMed PMID: ; PubMed Central PMCID: PMCPMC4319523. [PubMed: 25208284]

22. Wolf FJ, Grand DJ, Machan JT, et al. Microwave ablation of lung malignancies: effectiveness, CT findings, and safety in 50 patients. Radiology. 2008 6;247(3):871–9. doi: 10.1148/radiol. 2473070996. PubMed PMID: . [PubMed: 18372457]

23. Dodd GD, 3rd, Dodd NA, Lanctot AC, et al. Effect of variation of portal venous blood flow on radiofrequency and microwave ablations in a blood-perfused bovine liver model. Radiology. 2013 4;267(1):129–36. doi: 10.1148/radiol.12120486. PubMed PMID: . [PubMed: 23297326]

24. Velez E, Goldberg SN, Kumar G, et al. Hepatic Thermal Ablation: Effect of Device and Heating Parameters on Local Tissue Reactions and Distant Tumor Growth. Radiology. 2016 Dec;281(3): 782–792. doi: 10.1148/radiol.2016152241. PubMed PMID: ; PubMed Central PMCID: PMCPMC5131835. [PubMed: 27409564]

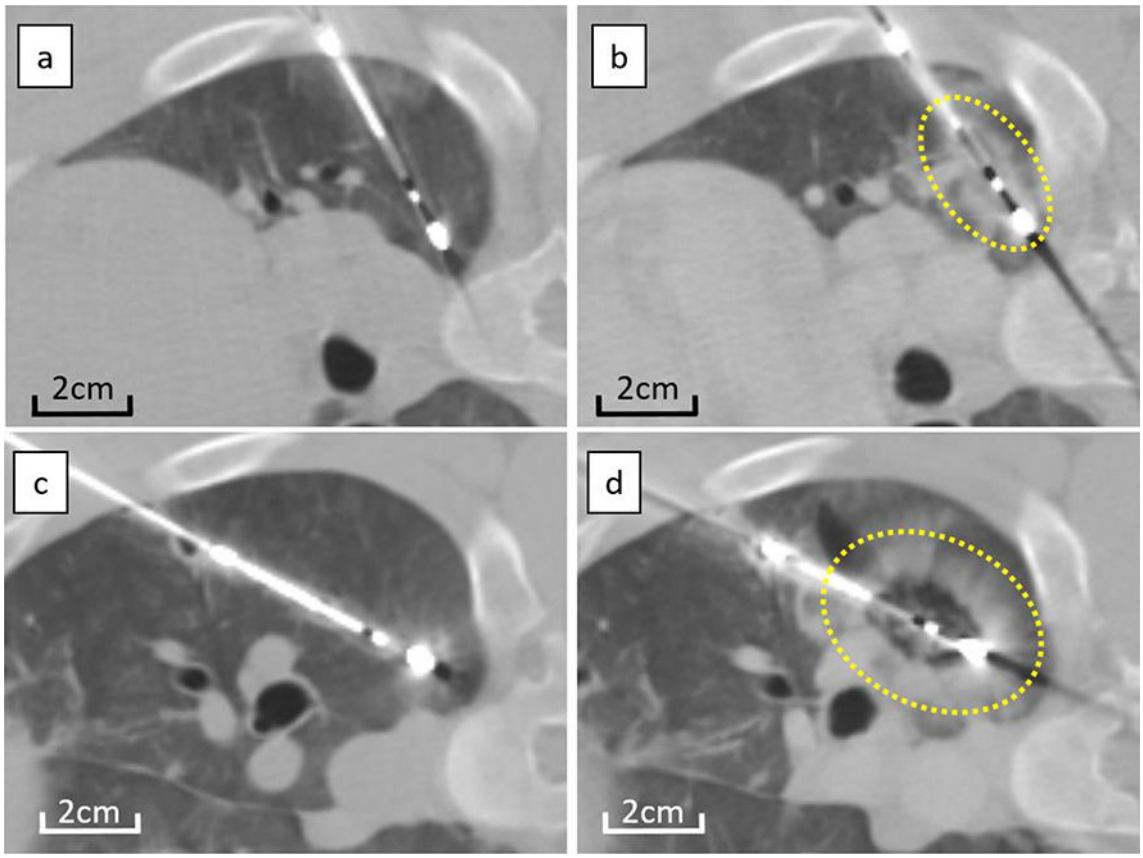


**Figure 1. Serial change of CT image following microwave ablation at high power**

CT images taken before ablation (a,c) and within 10 minutes after ablation (b,d) for short (a,b) and long (c,d) duration energy delivery. Compared to CT before ablation (a, c), low density area appeared around the electrode, surrounded by ill-demarcated consolidation on CT immediately after both short (b) and long duration (d) energy delivery. Ablation after long duration (d) treatment appears more spherical when compared to short duration (b) of energy delivery. Dotted lines demarcate the ablation zone from untreated lung.

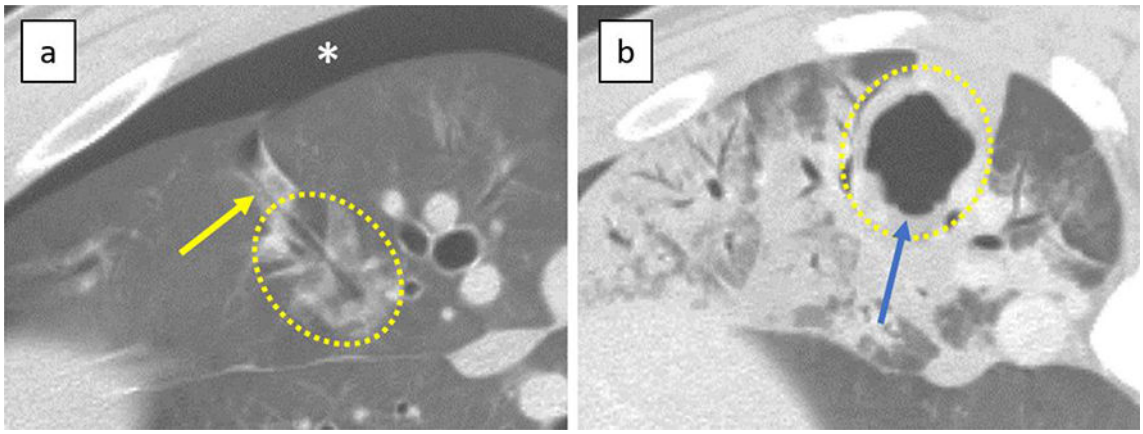


**Figure 2. Complications**

a) Pneumothorax; Pneumothorax appeared immediately after the removal of the antenna (*). This lesion was ablated with short duration of energy delivery. Air-filled needle tract connecting to pleural space (yellow arrow) was also visible. b) Cavitation within the ablation; Cavitation (blue arrow) was seen on CT at 7 days after the treatment and was completely enclosed with the ablation. This lesion was ablated with long duration of energy delivery. Dotted lines demarcate the ablation zone from untreated lung.

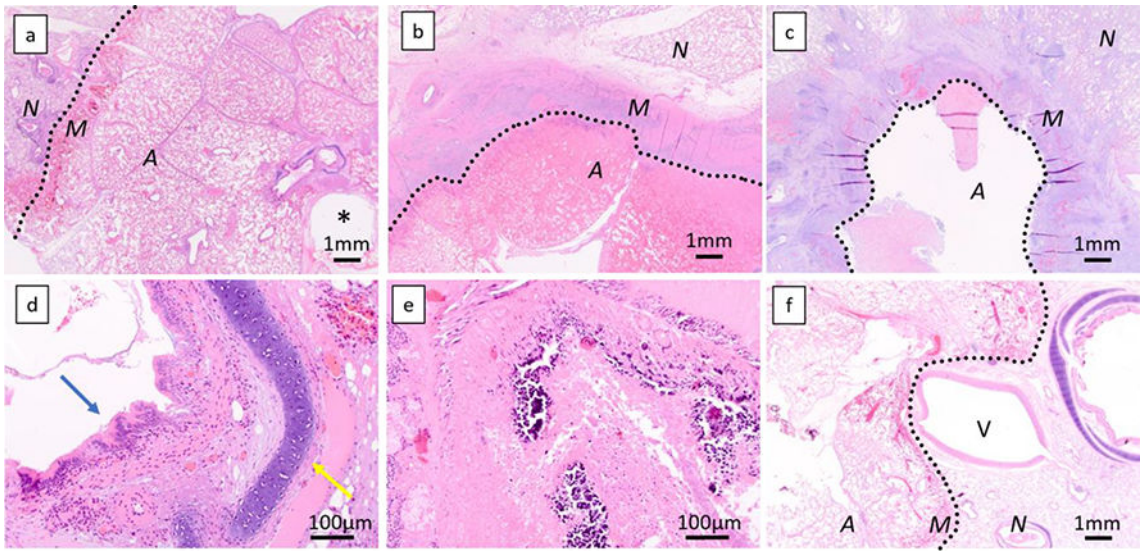


**Figure 3. Histology of ablation zone**

Histological specimen at day 2 (a, 1,25x, short duration) shows a well demarcated area of complete coagulation necrosis with a rim of hyperemia, hemorrhage, and fibrin exudation at the edge of the area of necrosis. At day 28, a rim of dense fibrosis and inflammation characterized by infiltration by numerous neutrophils, macrophages, lymphocytes, and plasma cells is seen (b, 1.25x, long duration). Some lesions show cavitation within the dense rim (c, 1.25x, short duration). All bronchi were completely ablated inside the ablation zone. At day 2, the structure, including epithelium (blue arrow) or cartilage (yellow arrow) of bronchus is maintained (d, 20x, short duration energy delivery), but is destroyed at day 28 (e, 20x, short duration energy delivery). A 5mm pulmonary artery at the edge of the necrotic zone shows incomplete necrosis, and the ablation zone margin is concaved (f, 1.25x, short duration energy delivery). *A*, ablated area; *M*, ablation margin; *N*, non-ablated area; *, antenna tract; *V*, pulmonary vein. Dotted lines demarcate the ablation zone from untreated lung.

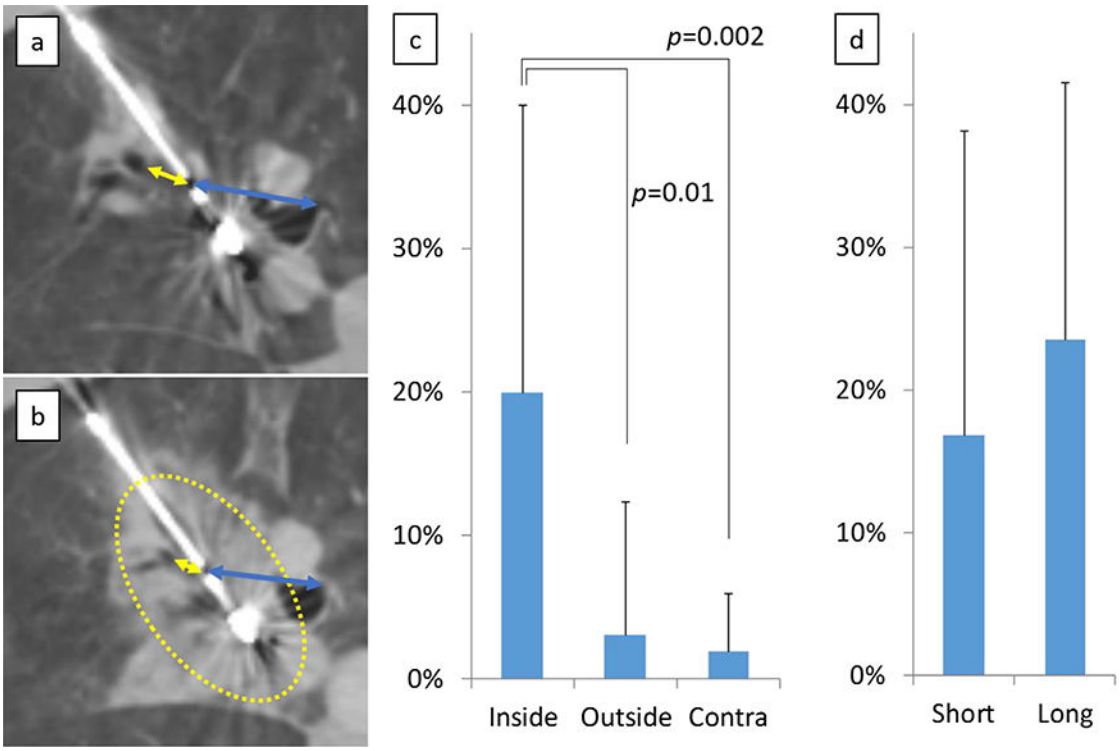


**Figure 4. Distortion of lung tissue following high power microwave ablation**

Distances between the center of the ablation zone, and bronchus or large vessels both inside (yellow arrow) and outside (blue arrow) the ablation zone were measured on CT images before (a) and immediately after ablation (b). The distance between the ablation center and these structures decreased significantly within the ablation when compared with structures outside the ablation zone, or equivalent measurements performed in untreated contralateral lung. (c). The distortion ratio between short (2 min) and long duration (10 min) was not significantly different (d). Dotted lines demarcate the ablation zone from untreated lung.

**Table 1:**

Adverse Event Results

| Animal No. | No. of ablation | | Follow-up (days) | Complication | | |
|---|---|---|---|---|---|---|
| | High dose (100W/10min) | Low dose (100W/2min) | | SIR criteria | Severity | Details |
| 1 | 1 | 1 | 2 | C | Major | Pneumothorax requiring chest tube |
| 2 | 1 | 1 | 2 | A | Minor | Pneumothorax |
| 3 | 1 | 2 | 28 | A | Minor | Pneumothorax |
| 4 | 1 | 2 | 28 | - | | |
| 5 | 1 | 2 | 28 | A | Minor | Pneumothorax |
| 6 | 1 | 2 | 0 | C or more | Major | Pneumothorax requiring chest tube |
| 7 | 1 | 2 | 28 | A | Minor | Pneumothorax |
| 8 | 1 | 2 | 28 | B | Minor | Pneumothorax with pneumonia |
| 9 | 1 | 2 | 28 | B | Minor | Cavitation at ablation site with pneumonia |
| 10 | 0 | 2 | | C or more | Major | Pneumothorax requiring chest tube |
| | Total | | | | | Major complication rate: 30% (3/10) |
| | 9 | 18 | | | | Minor Complication rate: 60% (6/10) |

**Table 2:**

CT findings at day 0

| | Short duration | Long duration | p-value |
|---|---|---|---|
| Air-filled needle tract | | | |
| Yes | 3 | 2 | NS |
| No | 15 | 7 | |
| Passage of air through needle tract to pleural cavity | | | |
| Yes | 1 | 1 | NS |
| No | 17 | 8 | |
| Long-axis diameter (cm) | | | |
| Mean±SD | 2.4±0.5 | 3.3±0.4 | <0.001 |
| Range | 1.4–3.4 | 2.6–3.8 | |
| Short-axis diameter (cm) | 1.3±0.4 | | |
| Mean±SD | | 2.3±0.3 | <0.001 |
| Range | 0.7–2.0 | 1.7–2.9 | |
| Volume ($cm^3$) | | | |
| Mean±SD | 3.4±1.7 | 8.9±3.1 | <0.001 |
| Range | 1.3–6.9 | 3.7–12.5 | |
| Sphericity | | | |
| Mean±SD | 0.56±0.13 | 0.70±0.10 | 0.01 |
| Range | 0.34–0.74 | 0.56-0.85 | |
| Distortion ratio (%) | | | |
| Mean±SD | 18±22 | 24±18 | NS |
| Range | 4–67 | 5–45 | |

**Table 3:**

Histological findings at day 2 and 28

| | Short duration | Long duration | p-value |
|---|---|---|---|
| Day 2 | | | |
| Airways within Ablation (Complete Necrosis) (mm) | | | |
| Mean±SD | 3.2±1.5 | 2.5±1.3 | NS |
| Range | 0.6–5.1 | 0.7–3.7 | |
| Vessels within Ablation (Complete Necrosis) (mm) | | | |
| Mean±SD | 1.5±1.2 | 2.5±1.1 | NS |
| Range | 0.2–3.3 | 1.9–4.1 | |
| Airways at Ablation Boundary (Incomplete Necrosis) (mm) | | | |
| Mean±SD | 2.0±2.0 | 2.8±3.0 | NS |
| Range | 0.3–5.5 | 0.6–7.2 | |
| Vessels at Ablation Boundary (Incomplete Necrosis | | | |
| Mean±SD | 2.5±1.1 | 1,5±1.2 | NS |
| Range | 0.5–3.1 | 1.0–4.0 | |
| Width of hyperemic rim (mm) | | | |
| Mean±SD | | 2.6±0.9 | |
| Range | 1.5–3.3 | 1.8–3.7 | NS |
| Day 28 | | | |
| Width of fibrotic rim (mm) | | | |
| Mean±SD | 1.9±0.6 | 2.1 ±0.1 | NS |
| Range | 1.0–2.5 | 2.0–2.2 | |